# The ASTRO-H Mission

Tadayuki Takahashi[a], Kazuhisa Mitsuda[a], Richard Kelley[b], Felix Aharonian[c], Fumie Akimoto[d], Steve Allen[e], Naohisa Anabuki[f], Lorella Angelini[b], Keith Arnaud[g], Hisamitsu Awaki[h], Aya Bamba[c], Nobutaka Bando[a], Mark Bautz[i], Roger Blandford[e], Kevin Boyce[b], Greg Brown[j], Maria Chernyakova[c], Paolo Coppi[k], Elisa Costantini[l], Jean Cottam[b], John Crow[b], Jelle de Plaa[l], Cor de Vries[l], Jan-Willem den Herder[l], Michael DiPirro[b], Chris Done[m], Tadayasu Dotani[a], Ken Ebisawa[a], Teruaki Enoto[e], Yuichiro Ezoe[n], Andrew Fabian[o], Ryuichi Fujimoto[p], Yasushi Fukazawa[q], Stefan Funk[e], Akihiro Furuzawa[d], Massimiliano Galeazzi[r], Poshak Gandhi[a], Keith Gendreau[b], Kirk Gilmore[e], Yoshito Haba[d], Kenji Hamaguchi[g], Isamu Hatsukade[s], Kiyoshi Hayashida[f], Junko Hiraga[t], Kazuyuki Hirose[a], Ann Hornschemeier[b], John Hughes[u], Una Hwang[v], Ryo Iizuka[w], Kazunori Ishibashi[d], Manabu Ishida[a], Kosei Ishimura[a], Yoshitaka Ishisaki[n], Naoki Isobe[x], Masayuki Ito[y], Naoko Iwata[a], Jelle Kaastra[l], Timothy Kallman[b], Tuneyoshi Kamae[e], Hideaki Katagiri[q], Jun Kataoka[z], Satoru Katsuda[b], Madoka Kawaharada[a], Nobuyuki Kawai[aa], Shigeo Kawasaki[a], Dmitry Khangaluyan[a], Caroline Kilbourne[b], Kenzo Kinugasa[ab], Shunji Kitamoto[ac], Tetsu Kitayama[ad], Takayoshi Kohmura[ae], Motohide Kokubun[a], Tatsuro Kosaka[af], Taro Kotani[ag], Katsuji Koyama[ah], Aya Kubota[ai], Hideyo Kunieda[d], Philippe Laurent[aj], François Lebrun[aj], Olivier Limousin[aj], Michael Loewenstein[b], Knox Long[ak], Grzegorz Madejski[e], Yoshitomo Maeda[a], Kazuo Makishima[t], Maxim Markevitch[al], Hironori Matsumoto[d], Kyoko Matsushita[am], Dan McCammon[an], Jon Miller[ao], Shin Mineshige[x], Kenji Minesugi[a], Takuya Miyazawa[d], Tsunefumi Mizuno[q], Koji Mori[s], Hideyuki Mori[a], Koji Mukai[b], Hiroshi Murakami[ac], Toshio Murakami[p], Richard Mushotzky[g], Yujin Nakagawa[ap], Takao Nakagawa[a], Hiroshi Nakajima[f], Takeshi Nakamori[z], Kazuhiro Nakazawa[t], Yoshiharu Namba[aq], Masaharu Nomachi[ar], Steve O' Dell[aw], Hiroyuki Ogawa[a], Mina Ogawa[a], Keiji Ogi[as], Takaya Ohashi[n], Masanori Ohno[a], Masayuki Ohta[a], Takashi Okajima[v], Naomi Ota[am], Masanobu Ozaki[a], Frits Paerels[at], Stéphane Paltani[au], Arvind Parmer[av], Robert Petre[b], Martin Pohl[au], Scott Porter[b], Brian Ramsey[aw], Christopher Reynolds[g], Shin-ichiro Sakai[a], Rita Sambruna[b], Goro Sato[a], Yoichi Sato[ax], Peter Serlemitsos[b], Maki Shida[a], Takanobu Shimada[a], Keisuke Shinozaki[ax], Peter Shirron[b], Randall Smith[al], Gary Sneiderman[b], Yang Soong[b], Lukasz Stawarz[a], Hiroyuki Sugita[ax], Andrew Szymkowiak[k], Hiroyasu Tajima[e], Hiromitsu Takahashi[q], Yoh Takei[a], Toru Tamagawa[ap], Takayuki Tamura[a], Keisuke Tamura[a], Takaaki Tanaka[e], Yasuo Tanaka[a], Yasuyuki Tanaka[a], Makoto Tashiro[ay], Yuzuru Tawara[d], Yukikatsu Terada[ay], Yuichi Terashima[h], Francesco Tombesi[b], Hiroshi Tomida[a], Miyako Tozuka[am], Yoko Tsuboi[w], Masahiro Tsujimoto[a], Hiroshi Tsunemi[f], Takeshi Tsuru[ah], Hiroyuki Uchida[f], Yasunobu Uchiyama[e], Hideki Uchiyama[t], Yoshihiro Ueda[x], Shinichiro Uno[az], Meg Urry[ba], Shin Watanabe[a], Nicholas White[b], Takahiro Yamada[a], Hiroya Yamaguchi[ap], Kazutaka Yamaoka[ag], Noriko Yamasaki[a], Makoto Yamauchi[s], Shigeo Yamauchi[bb], Yoichi Yatsu[aa], Daisuke Yonetoku[p], Atsumasa Yoshida[ag]

[a] Institute of Space and Astronautical Science (ISAS), JAXA, Kanagawa, 252-5210, Japan; [b] NASA/Goddard Space Flight Center, Greenbert, MD 20771, USA; [c]Dublin Institute for Advanced Studies, Dublin 2, Ireland; [d]Department of Physics, Nagoya University, Nagoya, 338-8570, Japan; [e]Kavli Institute for Particle Astrophysics and Cosmology, Stanford

University, CA 94305, USA; [f]Department of Earth and Space Science, Osaka University, Osaka, 560-0043, Japan; [g]Department of Physics, University of Maryland, MD 21250, USA; [h]Department of Physics, Ehime University, Ehime, 790-8577, Japan; [i]Kavli Institute for Astrophysics and Space Research, Massachusetts Institute of Technology, Cambridge, MA 02139, USA; [j]Lawrence Livermore National Laboratory, CA, 94550, USA; [k]Department of Physics, Yale University, CT 06520-8120, USA; [l]SRON Netherlands Institute for Space Research, Utrecht, the Netherlands; [m]Department of Physics, University of Durham, DH1 3LE, UK; [n]Department of Physics, Tokyo Metropolitan University, Tokyo, 192-0397, Japan; [o]Institute of Astronomy, Cambridge University, CB3 0HA, UK; [p] Faculty of Mathematics and Physics, Kanazawa University, Ishikawa, 920-1192, Japan; [q] Department of Physical Science, Hiroshima University, Hiroshima , 739-8526, Japan; [r] Physics Department, University of Miami, FL 33124, USA; [s]Department of Applied Physics, University of Miyazaki, Miyazaki, 889-2192, Japan; [t]Department of Physics, University of Tokyo, Tokyo, 113-0033, Japan; [u]Department of Physics and Astronomy, Rutgers University, NJ 08854-8019, USA; [v]Department of Physics and Astronomy, Johns Hopkins University, MD 21218, USA; [w]Department of Physics, Chuo University, Tokyo 112-8551, Japan; [x]Department of Astronomy, Kyoto University, Kyoto 606-8502, Japan; [y] Faculty of Human Development, Kobe University, Hyogo, 657-8501, Japan; [z]Research Institute for Science and Engineering, Waseda University, Tokyo 169-8555, Japan; [aa] Department of Physics, Tokyo Institute of Technology, Tokyo 152-8551, Japan; [ab]Gunma Astronomical Observatory, Gunma 377-0702, Japan; [ac]Department of Physics, Rikkyo University,Tokyo 171-8501, Japan; [ad]Department of Physics, Toho University, Chiba 274-8510, Japan; [ae]Department of Physics, Kougakuin University, Hachioji, Tokyo 192-0015, Japan; [af]School of Systems Engineering, Kochi University of Technology, Kochi 782-8502, Japan; [ag]Department of Physics and Mathematics, Aoyama Gakuin University, Kanagawa 229-8558, Japan; [ah]Department of Physics, Kyoto University, Kyoto, 606-8502, Japan; [ai]Department of Electronic Information Systems, Shibaura Institute of Technology, Saitama 337-8570, Japan; [aj]IRFU/Service d'Astrophysique, CEA Saclay, 91191 Gif-sur-Yvette, Cedex France; [ak]Space Science Telescope Institute, Baltimore, MD 21218 USA; [al]Harvard-Smithsonian Center for Astrophysics, MA 02138, USA; [am]Department of Physics, Tokyo University of Science, Tokyo, 162-8601, Japan; [an]Department of Physics, University of Wisconsin, WI 53706, USA; [ao]Department of Astronomy, University of Michigan, Ann Arbor, MI 48109; [ap]RIKEN, Saitama 351-0198, Japan; [aq]Department of Mechanical Engineering, Chubu University, Kasugai, Aichi 487-8501, Japan; [ar]Laboratory of Nuclear Studies, Osaka University, Osaka, 560-0043, Japan; [as]Graduate School of Science and Engineering,Ehime University, Ehime, 790-8577, Japan; [at]Columbia Astrophysics Laboratory, Department of Astronomy, Columbia University, NY 10027, USA [au]Université de Genève, Switzerland; [av]ESTEC, Space Science Dept., Noordwijk, The Netherlands; [aw]NASA/Marshall Space Flight Center, AL 35812, USA; [ax]Aerospace Research and Development Directorate, JAXA, Ibaraki, 305-8505, Japan; [ay]Department of Physics, Saitama University, Saitama, 338-8570, Japan; [az]Faculty of Social and Information Sciences, Nihon Fukushi University, Aichi 475-0012, Japan; [ba]Yale Center for Astronomy and Astrophysics, Yale University, New Haven, CT 06520-8121, USA; [bb]Department of Physics, Faculty of Science, Nara Women's University, Nara, Nara 630-8506, Japan;

## ABSTRACT

The joint JAXA/NASA ASTRO-H mission is the sixth in a series of highly successful X-ray missions initiated by the Institute of Space and Astronautical Science (ISAS). ASTRO-H will investigate the physics of the high-energy universe by performing high-resolution, high-throughput spectroscopy with moderate angular resolution. ASTRO-H covers very wide energy range from 0.3 keV to 600 keV. ASTRO-H allows a combination of wide band X-ray spectroscopy (5–80 keV) provided by multilayer coating, focusing hard X-ray mirrors and hard X-ray imaging detectors, and high energy-resolution soft X-ray spectroscopy (0.3–12 keV) provided by thin-foil X-ray optics and a micro-calorimeter array. The mission will also carry an X-ray CCD camera as a focal plane detector for a soft X-ray telescope (0.4–12 keV) and a non-focusing soft gamma-ray detector (40–600 keV) . The micro-calorimeter system is developed by an international collaboration led by ISAS/JAXA and NASA. The simultaneous broad bandpass, coupled with high spectral resolution of $\Delta E \sim 7$ eV provided by the micro-calorimeter will enable a wide variety of important science themes to be pursued.

**Keywords:** X-ray, Hard X-ray, Gamma-ray, X-ray Astronomy, Gamma-ray Astronomy, micro-calorimeter

## 1. INTRODUCTION

ASTRO-H, which was formerly called NeXT, is an international X-ray satellite that Japan plans to launch with the H-II A rocket in 2014.[1–5] NASA has selected the US participation in ASTRO-H as a Mission of Opportunity. Under this program, the NASA/Goddard Space Flight Center collaborates with ISAS/JAXA on the implementation of an X-ray micro-calorimeter spectrometer (SXS Proposal NASA/GSFC, 2007).[6] Other international members are from Stanford University, SRON, Geneva University and CEA/DSM/IRFU. In addition, in early 2009, NASA, ESA and JAXA have selected science working group members to provide scientific guidance to the ASTRO-H project relative to the design/development and operation phases of the mission.

The history and evolution of the Universe can be described as a process in which structures of different scales are formed such as stars, galaxies, and clusters of galaxies, but also as matter and energy concentrate to an extreme degree in a form of black holes and neutron stars. It is a mysery of Nature that the overwhelming diversity over tens or orders in spatial and density scales has been produced in the Universe following an expansion from a nearly uniform state. Clusters of galaxies are the largest astronomical object in the Universe. Observing clusters of galaxies and revealing their history is bound to lead to an understanding of how the structures are formed and evolved in the Universe. Equally important is to study how galaxies and supermassive black holes form and develop, and what role they play in forming clusters of galaxies.

About 80% of the observable matter in the Universe is thought be in a form of hot gas that can be directly studied only in the X-ray band. X-ray observations are indispensable for unveiling the mysteries of the Universe. The ASTRO-H mission is equipped with a suite of instruments with the highest energy resolution ever achieved at $E > 3$ keV and a wide energy range spanning four decades in energy from soft X-rays to gamma-rays. The mission aims to understand the dynamics of the evolution of the Universe and the concentration of the energy including how the most energetic particles, that are still far from thermal equilibrium, are produced.

ASTRO-H has just completed the preliminary design review (PDR) which is required before entering the detailed design phase (Phase C). In the PDR, the validity of various achievements in the basic design phase and the technical feasibility were examined. The review items included the effectiveness of the mission requirements at the time of the PDR and the validation of the development and verification plans. It was confirmed that the project is designed to ensure appropriate reliability to fulfill the mission goals as are listed in "the mission system requirement" document and that the project is feasible both technically and schedule-wise at the system, sub-systems, and component levels. Based on the results of the PDR, ASTRO-H is now in Phase C since May 2010.

In this paper, we will summarize the scientific requirements, the mission concept and the current baseline configuration of instruments of ASTRO-H.

ASTRO-H Web site: http://ASTRO-H.isas.jaxa.jp/index.html.en

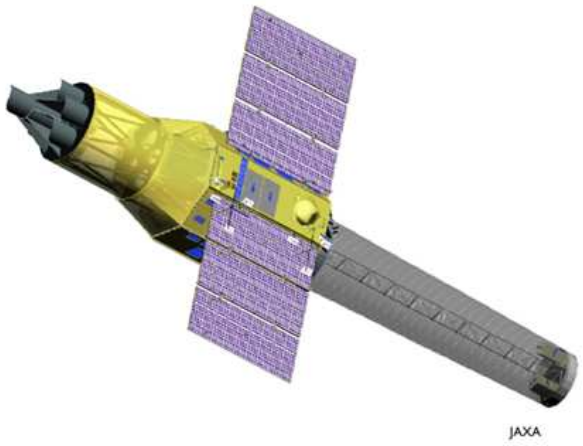


Figure 1. Artist's drawing of the ASTRO-H satellite. The focal length of the Hard X-ray Telescope (HXT) is 12m, whereas the Soft X-ray Spectrometer (SXS) and Soft X-ray Imager (SXI) will have a focal length of 5.6 meters.

Table 1. ASTRO-H Mission

| | |
|---|---|
| Launch site | Tanegashima Space Center, Japan |
| Launch vehicle | JAXA H-IIA rocket |
| Orbit Altitude | ∼550 km |
| Orbit Type | Approximate circular orbit |
| Orbit Inclination | $< 31$ degrees |
| Orbit Period | 96 minutes |
| Total Length | 14 m |
| Mass | $< 2.6$ metric ton |
| Power | $< 3500$ W |
| Telemetry Rate | 8 Mbps (X-band QPSK) |
| Recording Capacity | 12 Gbits at EOL |
| Mission life | $> 3$ years |

## 2. SCIENCE REQUIREMENTS

ASTRO-H aims to achieve the scientific goals and objectives listed below by inheriting the tradition and advancing the technology of highly successful X-ray missions initiated by SAS beginning with the launch of the Hakucho mission in 1979 through to the currently operating Suzaku mission.

### Scientific goals and Objectives

**Revealing the large-scale structure of the Universe and its evolution**

- ASTRO-H will observe clusters of galaxies, the largest bound structures in the Universe, with an aim to reveal the interplay between the thermal energy of the intracluster medium, the kinetic energy of sub-clusters from which clusters form, measure the non-thermal energy; and to directly trace the dynamic evolution of clusters of galaxies.
- ASTRO-H will observe distant supermassive black holes hidden by thick intervening material with 100 times higher sensitivity than Suzaku, and will study their evolution and role in galaxy formation.

**Understanding the extreme conditions in the Universe**

- ASTRO-H will measure the motion of matter very close to black holes with an aim to sense the gravitational distortion of space, and to understand the structure of relativistic space-time.

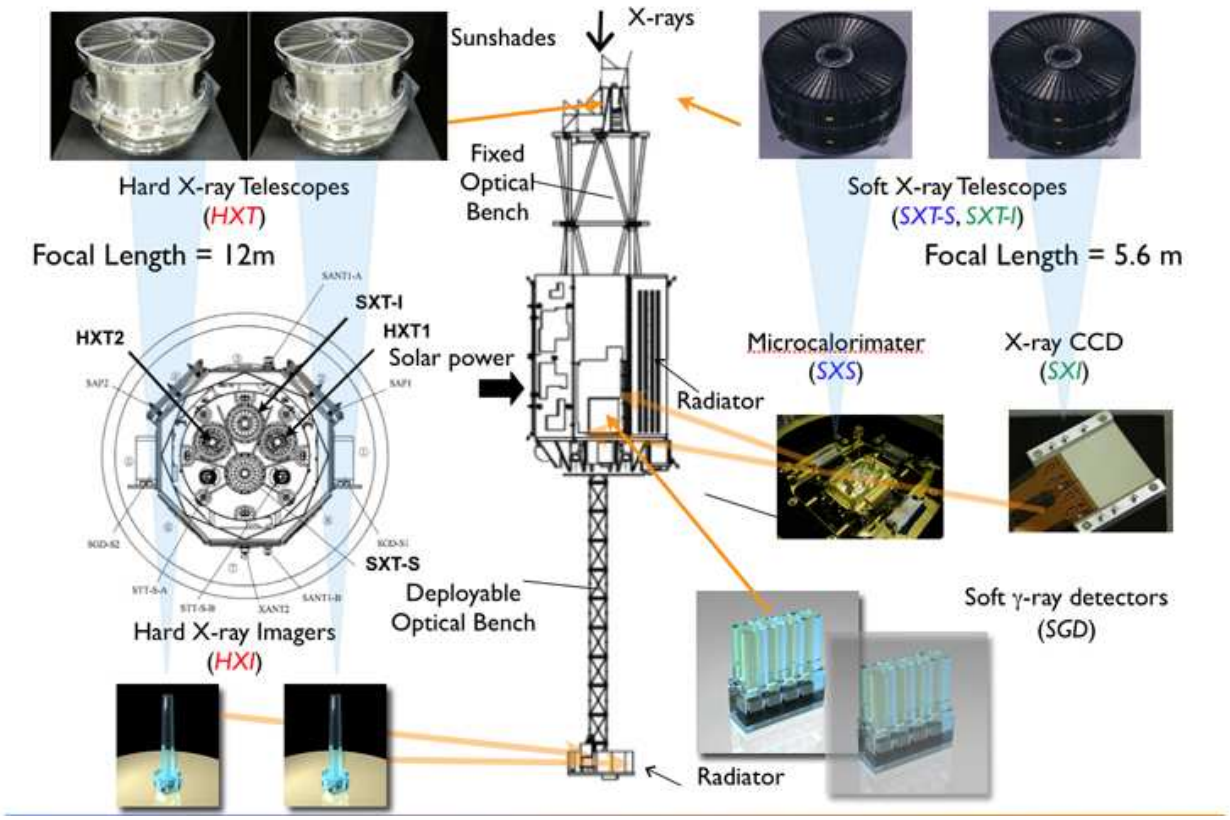


Figure 2. Configuration of the ASTRO-H satellite.

**Exploring the diverse phenomena of non-thermal Universe**

- ASTRO-H will derive the physical conditions of the sites where high energy particles (cosmic rays) gain energy and will elucidate the process in which gravity, collisions, and stellar explosions energize those cosmic rays.

**Elucidating dark matter and dark energy**

- ASTRO-H will map the distribution of dark matter in clusters of galaxies and will determine the total mass of galaxy clusters at different distances (and thus at different ages), and will study the role of dark matter and dark energy in the evolution of these systems.

In order to perform the leading edge science described above, ASTRO-H is designed with cutting edge technology. With an unprecedented spectroscopic capability and a wide-band energy coverage, ASTRO-H will measure the motion of hot gas, depicting the dynamic nature of the evolution of the Universe. These measurements will be the key in a great pursuit to understand the origin of the dark matter filling in the Universe.

## 3. SPACECRAFT AND INSTRUMENTS

ASTRO-H will carry two Hard X-ray Telescopes (HXTs) for the Hard X-ray Imager (HXI), and two Soft X-ray Telescopes (SXTs), one with a micro-calorimeter spectrometer array with excellent energy resolution of $\sim$7 eV, and the other with a large area CCD in their respective focal planes. In order to extend the energy coverage to the soft $\gamma$-ray region up to 600 keV, the Soft Gamma-ray Detector (SGD) will be implemented as a non-focusing detector. With these instruments, ASTRO-H will cover the bandpass between 0.3 keV and 600 keV. The conceptual design of each instrument is shown in Fig. 2 and the requirements and specifications

Table 2. Requirements to the instruments onboard ASTRO-H

| Science Payload | Energy Coverage | Requirements |
|---|---|---|
| Hard X-ray Imaging System : (HXT+HXI) | 5–80 keV | Sensitivity for detecting point sources with a brightness of 1/100,000 times fainter than the Crab nebula at >10 keV. Energy resolution to resolve background emission lines by activated material. |
| Soft X-ray Spectrometer System: (SXT-S+XCS) | 0.3–12 keV | Energy resolution corresponding to 300 km/s in the Doppler width of iron emission lines at 6 keV for representative clusters of galaxies. Fields of view covering 1/5 of the virial radius for representative clusters at a redshift of 0.1. |
| Soft X-ray Imaging System (SXT-I+SXI) | 0.4–12 keV | Fields of view twice as large as those of the Hard X-ray Imaging System and the Soft X-ray Spectrometer System for obtaining accurate wide energy range spectra and observing surrounding area of the main targets. |
| Soft $\gamma$-ray detector (SGD) | 40–600 keV | Sensitivity for obtaining spectra up to 600 keV for more than 10 point sources (spectral index of 1.7) with a brightness of 1/1,000 times fainter than the Crab nebula. |

of those instruments based on the base-line design are summarized in Table. 2 and 3. Detailed descriptions of the instruments are available in other papers in these proceedings.[7–12]

Both soft and hard X-ray mirrors are mounted on top of the fixed optical bench. The two focal-plane detectors for soft X-ray mirrors are mounted on the base plate of the spacecraft, while two hard X-ray detectors are mounted on the extensible optical bench to attain 12 m focal length.

ASTRO-H is in many ways similar to Suzaku in terms of orbit, pointing, and tracking capabilities, although the mass is considerably larger; the total mass at launch will be 2600 kg (compared with Suzaku's 1700 kg). ASTRO-H will be launched into a circular orbit with altitude 500–600 km, and inclination 31 degrees or less. Science operations will be similar to those of Suzaku, with pointed observation of each target until the integrated observing time is accumulated, and then slewing to the next target. A typical observation will require 40–100 ksec integrated observing time, which corresponds to 1–2.5 days of clock time. All instruments are co-aligned and will operate simultaneously.

### 3.1 Hard X-ray Imaging System

The hard X-ray imaging system onboard ASTRO-H consists of two identical mirror-detector pairs (HXT and HXI). The HXT has conical-foil mirrors with depth-graded multilayer reflecting surfaces that provide a 5–80 keV energy range.[11,13] The effective area of the HXT is maximized for a long focal length, with current design value of 12 m giving an effective area of $\sim$300 cm$^2$ at 30 keV for two HXTs. A depth-graded multilayer mirror reflects X-rays not only by total external reflection but also by Bragg reflection. In order to obtain high reflectivity up to 80 keV, the HXTs consist of a stack of multilayers with different sets of periodic length and number of layer pairs with a platinum/carbon coating. The technology of a hard X-ray focusing mirror has already been proved by the balloon programs InFOC$\mu$S (2001, 2004),[14,15] HEFT (2004)[16] and SUMIT (2006).[14]

The non-imaging instruments flown so far were essentially limited to studies of sources with 10–100 keV fluxes of at best $>4 \times 10^{-12}$–$10^{-11}$ erg cm$^{-2}$s$^{-1}$. This limitation is due to the presence of high un-rejected backgrounds from particle events and Cosmic X-ray radiation, which increasingly dominate above 10 keV. Imaging, and especially focusing instruments have two tremendous advantages. Firstly, the volume of the

Table 3. Specification of instruments

| | | |
|---|---|---|
| Hard X-ray Imaging System | HXT (Hard X-ray Telescope)/HXI (Hard X-ray Imager) | |
| | Focal Length | 12 m |
| | Effective Area | 300 $cm^2$ (at 30 keV) |
| | Energy Range | 5–80 keV |
| | Angular Resolution | <1.7 arcmin (HPD) |
| | Effective FOV | $\sim 9 \times 9$ arcmin (12 m Focal Length) |
| | Energy Resolution | $< 1.5$ keV (FWHM, at 60 keV) |
| | Timing Resolution | several 10 $\mu$s |
| | Detector Background | $< 1$–$3 \times 10^{-4}$ cts $s^{-1}$ $cm^{-2}$ $keV^{-1}$ |
| | Operating Temperature | $\sim -20$ °C |
| Soft X-ray Spectrometer System | SXT-S (Soft X-ray Telescope)/ XCS (X-ray Calorimeter Spectrometer) | |
| | Focal Length | 5.6 m |
| | Effective Area | 210 $cm^2$ (at 6 keV) |
| | | 160 $cm^2$ (at 1 keV) |
| | Energy Range | 0.3–12 keV |
| | Angular Resolution | $< 1.7$ arcmin (HPD) |
| | Effective FOV | $\sim 3 \times 3$ arcmin |
| | Energy Resolution | 7 eV (FWHM, at 6 keV) |
| | Timing Resolution | 80 $\mu$s |
| | Detector Background | $<6 \times 10^{-3}$ cts $s^{-1}$ $cm^{-2}$ $keV^{-1}$ |
| | Operating Temperature | 50 mK |
| Soft X-ray Imaging System | SXT-I (Soft X-ray Telescope)/SXI (Soft X-ray Imager) | |
| | Focal Length | 5.6 m |
| | Effective Area | 360 $cm^2$ (at 6 keV) |
| | Energy Range | 0.4–12 keV |
| | Angular Resolution | $< 1.7$ arcmin (HPD) |
| | Effective FOV | $\sim 38 \times 38$ arcmin |
| | Energy Resolution | $< 150$ eV (FWHM, at 6 keV) |
| | Timing Resolution | 4 sec |
| | Detector Background | $<$ a few $\times 10^{-3}$ cts $s^{-1}$ $cm^{-2}$ $keV^{-1}$ |
| | Operating Temperature | $-120$ °C |
| Soft Gamma-ray non-Imaging System | SGD (Soft Gamma-ray Detector) | |
| | Energy Range | a few 10 keV$-$600 keV |
| | Energy Resolution | $\sim 2$ keV (FWHM, at 40 keV) |
| | Geometrical Area | 210 $cm^2$ |
| | Effective Area | $\sim 30$ $cm^2$ (Compton mode, at 100 keV) |
| | FOV | $0.6 \times 0.6$ $deg^2$ ($< 150$ keV) |
| | Timing Resolution | several 10 $\mu$s |
| | Detector Background | $<$ a few $\times 10^{-6}$ cts $s^{-1}$ $cm^{-2}$ $keV^{-1}$ |
| | | ( 100–200 keV) |
| | Operating Temperature | $\sim -20$ °C |

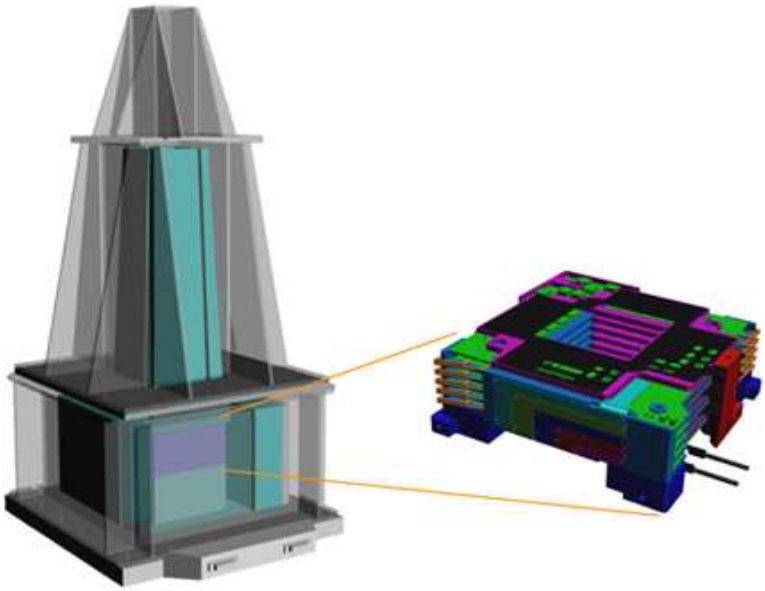

Figure 3. The Hard X-ray Imager. A stack of Si and CdTe double sided cross-strip detectors is mounted in a well-type BGO shield.

focal plane detector can be made much smaller than for non-focusing instruments, thus reducing the absolute background level since the background flux generally scales with the size of the detector. Secondly, the residual background, often time-variable, can be measured simultaneously with the source, and can be reliably subtracted. For these reasons, a focusing hard X-ray telescope in conjunction with an imaging detector sensitive for hard X-ray photons is the appropriate choice to achieve a breakthrough in sensitivity for the field of high energy astronomy. In addition to the improvement of sensitivity, the HXI provides a "true" imaging capability which enable us to study spatial distributions of hard X-ray emission.

The HXI consists of four-layers of 0.5 mm thick Double-sided Silicon Strip Detectors (DSSD) and one layer of 0.75 mm thick CdTe imaging detector (Fig. 3).[7,17–19] In this configuration, soft X-ray photons below $<\sim$ 20 keV are absorbed in the Si part (DSSD), while hard X-ray photons above $\sim$ 20 keV go through the Si part and are detected by the newly developed CdTe double sided cross-strip detector. The low energy spectrum, obtained with Si, is less contaminated by the background due to activation in heavy material, such as Cd and Te. Fast timing response of silicon strip detector and CdTe strip detector allows us to place the entire detector inside a very deep well of the active shield made of BGO ($Bi_4Ge_3O_{12}$) scintillators. Signal from the BGO shield is used to reject background events. The DSSDs cover the energy below 30 keV while the CdTe strip detector covers the 20–80 keV band. Each DSSD has a size of $3.2\times3.2$ cm$^2$ and a thickness of 0.5 mm, resulting in 2 mm in total thickness, the same as that of the PIN detector of the HXD onboard Suzaku. A CdTe strip detector has a size of $3.2\times3.2$ cm$^2$ and a thickness of 0.75 mm. In addition to the increase of efficiency, the stack configuration and individual readout provide information on the interaction depth. This depth information is very useful to reduce the background in space applications, because we can expect that low energy X-rays interact in the upper layers and, therefore, it is possible to reject the low energy events detected in lower layers. Moreover, since the background rate scales with the detector volume, low energy events collected from the first few layers in the stacked detector have a high signal to background ratio, in comparison with events obtained from a monolithic detector with a thickness equal to the sum of all layers.

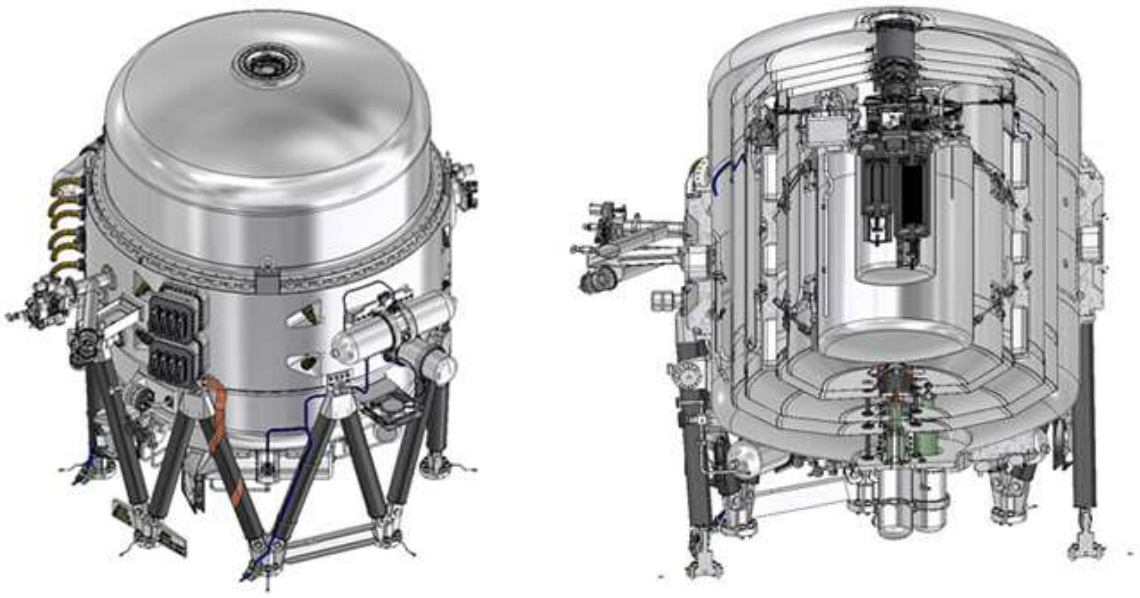

Figure 4. Outlook and cross sectional view of the SXS dewar. The outer shell of the dewar is 950 mm in diameter.

### 3.2 Soft X-ray Spectrometer System

The soft X-ray Spectrometer (SXS) consists of the Soft X-ray Telescope (SXT-S), the X-ray Calorimeter Spectrometer (XCS) and the cooling system.[8,20] The XCS is a 36 pixel system with an energy resolution of $\leq$7 eV between 0.3–12 keV. Micromachined, ion-implanted silicon is the basis of the thermistor array, and 8-micron-thick HgTe absorbers provide high quantum efficiency across the 0.3–12 keV band. With a 5.6-m focal length, the 0.83 mm pixel pitch corresponds to 0.51 arcmin, giving the array a field of view of 3.04 arcmin on a side. The detector assembly provides electrical, thermal, and mechanical interfaces between the detectors (calorimeter array and anti-coincidence particle detector) and the rest of the instrument. Soft X-ray Telescope (SXT) for XCS is an upgraded version of the Suzaku X-ray telescope with an improved angular resolution and a larger area.[12,21]

The SXS science objectives require a mirror with larger effective area than those flown on Suzaku, especially in the Fe K band. This is attained by the combination of increased focal length and larger diameter. The SXS effective area at 6 keV is 210 cm$^2$, a 60 % increase over the Suzaku XRS, while at 1 keV the SXS has 160 cm$^2$, a 20 % increase. The required angular resolution is 1.7 arcmin, HPD, comparable to the in-orbit performance of the mirrors on Suzaku.

The XCS cooling system must cool the array to 50 mK with sufficient duty cycle to fulfill the SXS scientific objectives: this requires extremely low heat loads. To achieve the necessary gain stability and energy resolution, the cooling system must regulate the detector temperature to within 2 $\mu$K rms for at least 24 hours per cycle. From the detector stage to room temperature, the cooling chain is composed of a 3-stage Adiabatic Demagnetization Refrigerator (ADR), superfluid liquid $^4$He (hereafter LHe), a $^4$He Joule-Thomson (JT) cryocooler, and 2-stage Stirling cryocoolers. As with Suzaku, the array will be cooled using an ADR.[22,23] An ADR has been adopted because it readily meets the requirements for detector temperature, stability, recycle time, reliability in a space environment, and previous flight heritage. The design of Stirling cryocoolers is based on coolers developed for space-flight missions in Japan (Suzaku, AKARI, and the SMILES instrument deployed on the ISS[24]) that have achieved excellent performance with respect to cooling power, efficiency and mass. As a heat-sink for the 2-stage ADR, 30 L of LHe is used. To reduce the parasitic heat load on the He tank, a $^4$He JT cryocooler is used to cool a 4 K shield. To achieve redundancy for failure (unexpected loss) of LHe, another ADR (3rd stage ADR) is used between the He tank and the JT cryocooler, with two heat-switches on both sides. This ADR is operated if LHe is lost, to cool down the 1 K shield (He tank). A series of five blocking filters shield the calorimeter array from UV

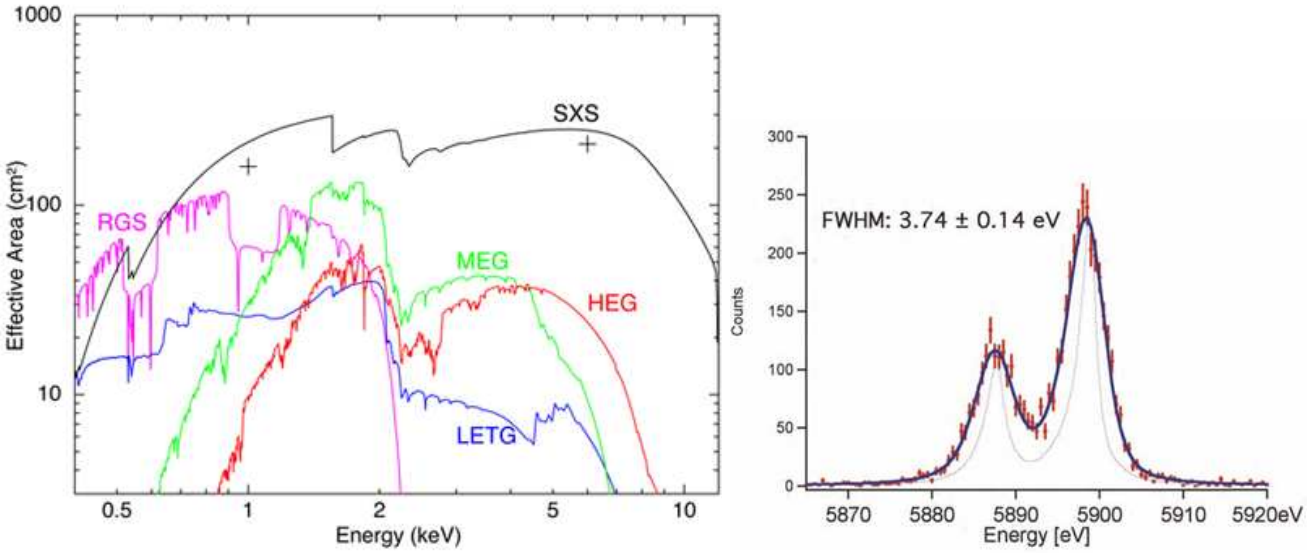


Figure 5. (left) The effective area of SXS (right). The energy resolution obtained from Mn K$\alpha_1$ using a detector from the XRS program but with a new sample of absorber material (HgTe) that has lower specific heat, leading to an energy resolution of 3.7 eV (FWHM). The SXS could have an energy resolution approaching this value.[26–28]

and longer wavelength radiation. The aluminized polyimide filters are similar to those successfully flown on Suzaku.

In combination with a high throughput X-ray telescope, the SXS improves on the Chandra and XMM-Newton grating spectrometers in two important ways. At E > 2 keV, SXS is both more sensitive and has higher resolution (Fig.5), especially in the Fe K band where SXS has 10 times the collecting area and much better energy resolution, giving a net improvement in sensitivity by a factor of 30 over Chandra. The broad bandpass of the SXS encompasses the critical inner-shell emission and absorption lines of Fe I-XXVI between 6.4 and 9.1 keV. Fe K lines provide particularly useful diagnostics because of their (1) strength, due to the high abundance and large fluorescent yield (30%), (2) spectral isolation from other lines, and (3) relative simplicity of the atomic physics. Fe K emission lines reveal conditions in plasmas with temperatures between $10^7$ and $10^8$ K, which are typical values for stellar accretion disks, SNRs, clusters of galaxies, and many stellar coronae. In cooler plasmas, Si, S, and Fe fluorescence and recombination occurs when an X-ray source illuminates nearby neutral material. Fe emission lines provide powerful diagnostics of non-equilibrium ionization due to inner shell K-shell transitions from Fe XVII–XXIV.[29]

In order to obtain a good performance for bright sources, a filter wheel (FW) assembly, which includes a wheel with selectable filters and a set of modulated X-ray sources will be used at a distance of 90 cm from the detector. The FW is able to rotate a suitable filter into the beam to optimize the quality of the data, depending on the source characteristics.[25] In addition to the filters, a set of on-off-switchable X-ray calibration sources, using light sensitive photo-cathode, will be implemented. These calibration sources will allow proper gain and linearity calibration of the detector in flight.

SXS uniquely performs high-resolution spectroscopy of extended sources. In contrast to a grating, the spectral resolution of the calorimeter is unaffected by source's angular size because it is non-dispersive. For sources with angular extent larger than 10 arcsec, Chandra MEG energy resolution is degraded compared with that of a CCD; the energy resolution of the XMM-Newton RGS is similarly degraded for sources with angular extent $\geq$2 arcmin. SXS makes possible high-resolution spectroscopy of sources inaccessible to current grating instruments.

The key properties of SXS are its high spectral resolution for both point and diffuse sources over a broad bandpass ($\leq$7 eV FWHM throughout the 0.3–12 keV band), high sensitivity (effective area of 160 cm$^2$ at 1 keV and 210 cm$^2$ at 7 keV), and low non-X-ray background ($1.5\times10^{-3}$ cts s$^{-1}$keV$^{-1}$). These properties

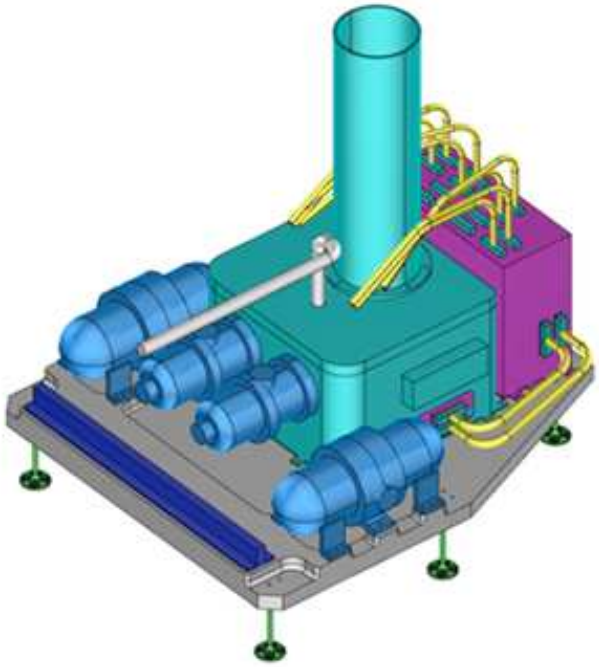

Figure 6. Schematic drawing of the Soft X-ray Imager (SXI and a picture of a prototype CCD chip).

open up a full range of plasma diagnostics and kinematic studies of X-ray emitting gas for thousands of targets, both Galactic and extragalactic. SXS improves upon and complements the current generation of X-ray missions, including Chandra, XMM-Newton, Suzaku and Swift.

### 3.3 Soft X-ray Imaging System

X-ray sensitive silicon charge-coupled devices (CCDs) are a key device for the X-ray astronomy. The low background and high energy resolution achieved with the XIS/Suzaku clearly show that the X-ray CCD will also play very important role in the ASTRO-H mission. Soft X-ray imaging system will consist of an imaging mirror and a CCD camera (Soft X-ray Telescope (SXT-I) and Soft X-ray Imager (SXI)).[9,30,31] Fig. 6 shows an schematic drawing of SXI.

In order to cover the soft X-ray band below 12 keV, the SXI will use next generation Hamamatsu CCD chips with a thick depletion layer of 200 $\mu$m, low noise, and almost no cosmetic defects. The SXI features a large FOV and covers a 38×38 arcmin$^2$ region on the sky, complementing the smaller FOV of the SXS calorimeter. A mechanical cooler ensures a long operational life at $-120$ °C. The overall quantum efficiency and spectral resolution is better than the Suzaku XIS. The imaging mirror has a 5.6-m focal length, and a diameter of 45 cm.

### 3.4 Soft Gamma-ray Detector (SGD)

Highly sensitive observations in the energy range above the HXT/HXI bandpass are crucial to study the spectrum of X-rays arising from accelerated particles. The SGD is a non-focusing soft gamma-ray detector with a 40–600 keV energy range and sensitivity at 300 keV of more than 10 times better than the Suzaku HXD (Hard X-ray Detector). It outperforms previous soft-$\gamma$-ray instruments in background rejection capability by adopting a new concept of narrow-FOV Compton telescope.[32,33]

In order to lower the background dramatically and thus to improve the sensitivity as compared to the HXD of Suzaku, the design combines a stack of Si and CdTe pixel detectors to form a Compton camera. The telescope is then mounted inside the bottom of a well-type active shield. Above $\sim$40 keV, each valid event is required to interact twice in the stacked detector, once by Compton scattering in a stack of Si strip detectors,

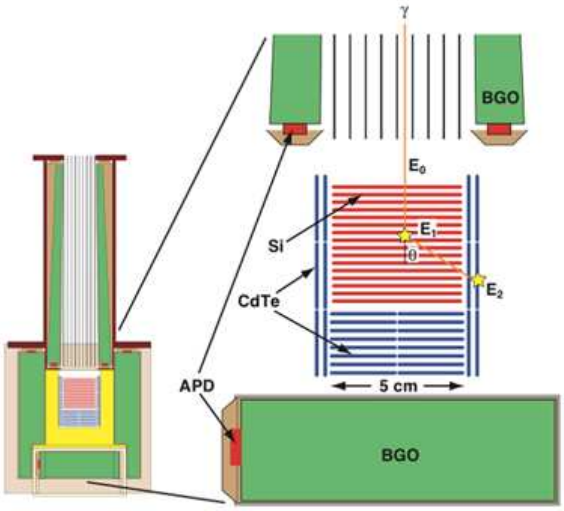


Figure 7. Conceptual drawing of an SGD Compton camera unit.

and then by photo-absorption in the CdTe part (Compton mode). Once the locations and energies of the two interactions are measured, the Compton kinematics allows the calculation of the energy and direction (as a cone in the sky) of the incident $\gamma$-ray.

As shown schematically in Fig. 7, the telescope consists of 32 layers of 0.6 mm thick Si pad detectors and eight layers of CdTe pixellated detectors with a thickness of 0.75 mm. The sides are also surrounded by two layers of CdTe pixel detectors. The opening angle provided by the BGO shield is $\sim$10 degrees at 500 keV. As compared to the HXD, the shield part is made compact by adopting the newly developed avalanche photo-diode. An additional PCuSn collimator restricts the field of view of the telescope to 30' for photons below 100 keV to minimize the flux due to the Cosmic X-ray Background in the FOV. These modules are then arrayed to provide the required area.

ASTRO-H will have two SGD detectors, each consisting of four units. Each detector will be mounted separately on two sides of the satellite. It should be noted that when the Compton condition is not used (Photo absorption mode), the stacked DSSD can be used as a standard photo-absorption type detector with the total thickness $\sim$20 mm of silicon. The detector then covers energies above 10 keV as a collimated-type $\gamma$-ray detector. The effective area of the SGD is $>$30 cm$^2$ at 100 keV in the Compton mode. Since the scattering angle of gamma-rays can be measured via reconstruction of the Compton scattering in the Compton camera, the SGD is capable of measuring polarization of celestial sources brighter than a few $\times$ 1/100 of the Crab Nebula, polarized above $\sim$ 10 %. This capability is expected to yield polarization measurements in several celestial objects, providing new insights into properties of soft gamma-ray emission processes.[10,34]

## 4. EXPECTED SCIENTIFIC PERFORMANCE

The ASTRO-H mission objectives are: to study the evolution of yet-unknown obscured supermassive black holes (SMBHs) in Active Galactic Nuclei (AGN); to trace the growth history of the largest structures in the Universe; to provide insights into the behavior of material in extreme gravitational fields; to determine the spin of black holes and the equation of state of neutron stars; to trace particle acceleration structures in clusters of galaxies and SNRs; and to investigate the detailed physics of astrophysical jets.

With ASTRO-H, we expect to achieve an area of about 300 cm$^2$ at 30 keV with a typical angular resolution of 1.7 arcmin (HPD). Fig. 8 shows detection limits of the SXT-I/SXI, HXT/HXI and SGD for point sources and for sources with of $1 \times 1$ deg$^2$ extension.

The imaging capabilities at high X-ray energies open the completely new field of spatial studies of non-thermal emission above 10 keV. This will enable us to track the evolution of active galaxies with

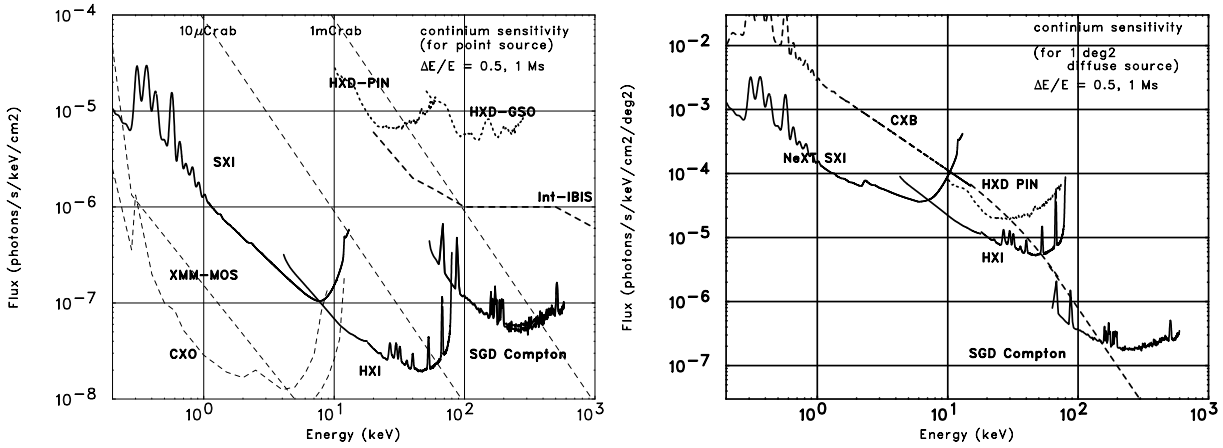


Figure 8. Detection limits of the SXT-I/SXI, HXT/HXI and SGD for (a) point sources and (b) for sources with of $1\times1$ deg$^2$ extension (bottom) as functions of X-ray energy, where the spectral binning with $\Delta E/E = 0.5$ and 1000 ksec exposure are assumed. Detection limits for the XMM-Newton, Chandra, Suzaku and Integral observatories are shown for comparison for the sensitivity for point sources.

accretion flows which are heavily obscured, in order to accurately assess their contribution to the cosmic X-ray background over cosmic time. It will also uniquely allow mapping of the spatial extent of the hard X-ray emission in diffuse sources, thus tracing the sites of particle acceleration in structures ranging in size from clusters of galaxies down to supernova remnants.[35–37] Those studies will be complementary to the SXS measurements: observing the hard X-ray synchrotron emission will allow a study of the most energetic particles, thus revealing the details of particle acceleration mechanisms in supernova remnants, while the high resolution SXS data on the gas kinematics of the remnant will constrain the energy input into the accelerators.

SXS spectroscopy of extended sources can reveal line broadening and Doppler shifts due to turbulent or bulk velocities. This capability enables the spectral identification of cluster mergers, SNR ejecta dispersal patterns, the structure of AGN and starburst winds, and the spatially dependent abundance pattern in clusters and elliptical galaxies. SXS can also measure the optical depths of resonance absorption lines, from which the degree and spatial extent of turbulence can be inferred. Additionally, SXS can reveal the presence of relatively rare elements in SNRs and other sources through its high sensitivity to low equivalent width emission lines. The low SXS background ensures that the observations of almost all line rich objects will be photon limited rather than background limited.

### 4.1 Supernova Remnants

The high resolution X-ray spectroscopy provided by ASTRO-H will be particularly ground-breaking for supernova remnants (SNRs) because they are extended objects with rich emission-line spectra from a wide range of different elements (carbon through nickel). To determine the element abundances reliably, measurements of the relative strengths of a number of lines from each elemental species are required. Accurate element abundances provide constraints to test the explosion mechanisms of supernovae and to explore their environments. Gas motions of the rapidly expanding supernova ejecta and swept-up interstellar/circumstellar medium may also be measured by ASTRO-H via their Doppler shifts. Velocity measurements inferred from such Doppler shifts are needed to understand how SNRs evolve, based on their age and the detailed properties of the explosion, the ejecta, and ambient medium.

Particle acceleration is receiving much attention at present, but the origin of cosmic rays is still unclear 100 years after their discovery. Young SNRs with shock speeds of several 1000 km/s are among the best candidates to accelerate cosmic rays up to the knee around $10^{15}$ eV (the highest energy accessible to Galactic accelerators). The combination of ASTRO-H's hard X-ray imaging capability and high spectral resolution will provide information to understand crucial aspects of shock acceleration in SNRs such as the maximum

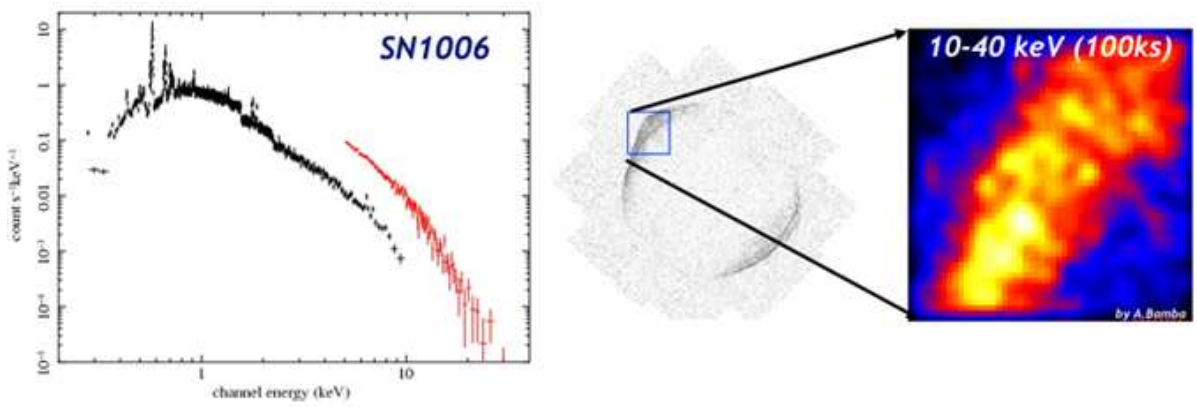


Figure 9. (left) Simulated spectra for 100 ks SXS observation of SN1006 with SXS and HXI. (right) Image expected from the combination of HXT and HXI.

energy of the accelerated particles, the conditions at the acceleration sites, and the acceleration efficiency (See Fig. 9).

### 4.2 A Census of Obscured Active Galactic Nuclei

Recent observations imply the existence of a large number of Active Galactic Nuclei (AGN) that are heavily obscured by the gas and dust surrounding their supermassive black holes.[38] Some are identified as a "new type" of AGN, so deeply buried in dense tori of gas that they show little emission in soft X-ray and visible light. While this has made such objects extremely difficult to detect and observe, this highly obscured activity may in fact represent the dominant phase of supermassive black hole growth. Understanding this phase is thus key to understanding the correlated evolution of the black hole and its host galaxy. As shown in Fig. 10, the high sensitivity for hard X-rays provided by HXI allows precise spectral studies of even very obscured AGN. ASTRO-H will provide us with a large AGN sample to pursue systematic studies of the true AGN population, unbiased by obscuration effects, and to measure the co-evolution of supermassive black holes with their host galaxies.

By assuming a background level of $\sim 1\times10^{-4}$ counts/s/cm$^2$/keV, in which the non X-ray background is dominant, the source detection limit in 1000 ksec in the $10-80$ keV band would be roughly $10^{-14}$ erg cm$^2$ s$^{-1}$ (for a power-law spectrum with a photon index of 2). This is about two orders of magnitude better than present instrumentation, and thus will result in a breakthrough in our understanding of hard X-ray spectra. With this sensitivity, 40-50 % of hard X-ray Cosmic Background would be be resolved[39] . In addition to the imaging observations below 80 keV, the SGD will provide a high sensitivity in the soft $\gamma$-ray region to match the sensitivity of the HXT/HXI combination. The extremely low background observations allowed by the new concept of a narrow-FOV Compton telescope adopted for the SGD will provide sensitive $\gamma$-ray spectra up to 600 keV, with moderate sensitivity for polarization measurements.

### 4.3 Close to Black Holes

On the smallest scales, many active galactic nuclei (AGN) show signatures from the innermost accretion disk in the form of broad "relativistic" Fe K emission lines. These broad lines were discovered using ASCA in the early 1990s and have been confirmed by XMM-Newton and Suzaku.[40,41] There is, however, a complex relationship between the Fe K line properties, the underlying continuum, and the signatures of cold and/or partially ionized material near the AGN. Precise measurements of the complex Fe K line and absorption components require high spectral resolution. The measurement of changes in the X-ray emission and absorption spectral features on the orbital time scale of black holes in AGN, will enable characterization of the velocity field and ionization state of the plasma closest to the event horizon. The optically thick material that produces the broad fluorescent Fe K line also creates a Compton "hump" peaking at $E > 20$ keV

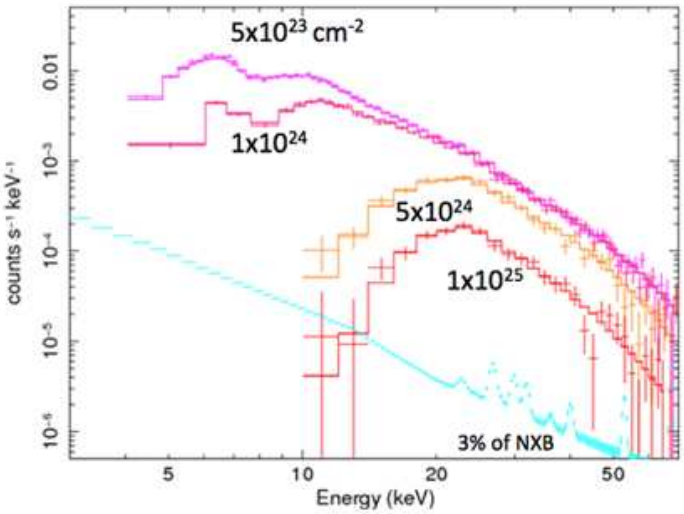


Figure 10. Simulated HXI spectra of heavily obscured AGN with different absorbing columns ($N_H$) for an exposure of 100 ks. The continuum is assumed to be a power-law of photon index 1.9, with an intrinsic 2-10 keV flux of $1x10^{-11}$ erg/cm$^2$/$s$ (based on Swift J0601.9-8636[38]). Scattered component and Fe lines are not included.

detectable with hard X-ray and soft gamma-ray detectors, providing multiple insights into the physics of the disk. In order to understand the evolution of environments surrounding supermassive black holes, high signal-to-noise measurements of the broad lines of many AGN are needed up to, at least, $z$∼2. This requires high spectral resolution and bandpass extending to at least ∼40 keV. These observations will provide the first unbiased survey of broad Fe K line properties across all AGN.

XMM-Newton and Suzaku spectra frequently show time-variable absorption and emission features in the 5–10 keV band. If these features are due to Fe, they represent gas moving at very high velocities with both red- and blue-shifted components from material presumably near the event horizon. CCD resolution is insufficient, and the required grating exposures are too long to properly characterize the velocity field and ionization of this gas and determine whether it is from close to the black hole or from high velocity winds. SXS, in combination with HXI, provides a dramatic increase in sensitivity over Suzaku, enabling measurements that probe the geometry of the central regions of ∼50 AGNs on the orbital timescale of the Fe producing region (for an AGN with a $3{\times}10^7 M_\odot$ black hole, this is ∼60 $GM/c^3$ = 10 ksec).

### 4.4 Clusters of Galaxies

All studies of the total energy content (including that of non-thermal particles), aimed to draw a more complete picture of the high energy universe, require observations by *both* a spectrometer capable of measuring the bulk plasma velocities and/or turbulence with the resolution corresponding to the speed of a few × 100 km/s *and* an arc-min imaging system in the hard X-ray band, with the sensitivity two-orders of magnitude better than previous missions (See Fig. 11 and Fig. 12). In clusters, X-ray emitting hot gas is trapped in the gravitational potential well and shocks and/or turbulence are produced in this gas, as smaller substructures with their own hot gas halos fall into and merge with the dominant cluster. Large scale shocks can also be produced as gas from the intracluster medium falls into the gravitational potential of a cluster. Here, there is a strong synergy between the hard X-ray imaging data and the high resolution (several eV) soft X-ray spectrometer which allows us to study the gas kinematics (bulk motion and turbulent velocity) via the width and energy of the emission lines. The kinematics of the gas provides unprecedented information about the bulk motion; the energy of this motion is in turn responsible for acceleration of particles to very high energies at shocks, which is in turn manifested via non-thermal processes, best studied via sensitive hard X-ray measurements.

Precision cosmology uses astronomical observations to determine the large-scale structure and content of the Universe. Studies of clusters of galaxies have provided independent measurements of the dark en-

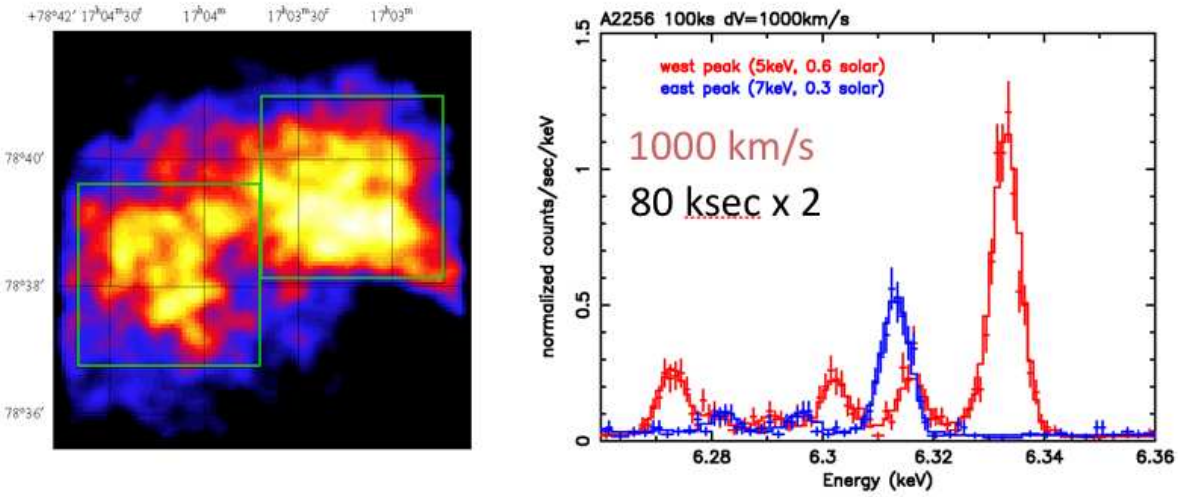


Figure 11. Simulated image and spectra of a merging cluster A2256 by assuming 1000 km/s difference of line of sight speed of hot gas in the cluster. The simulation is for 80 ksec each.

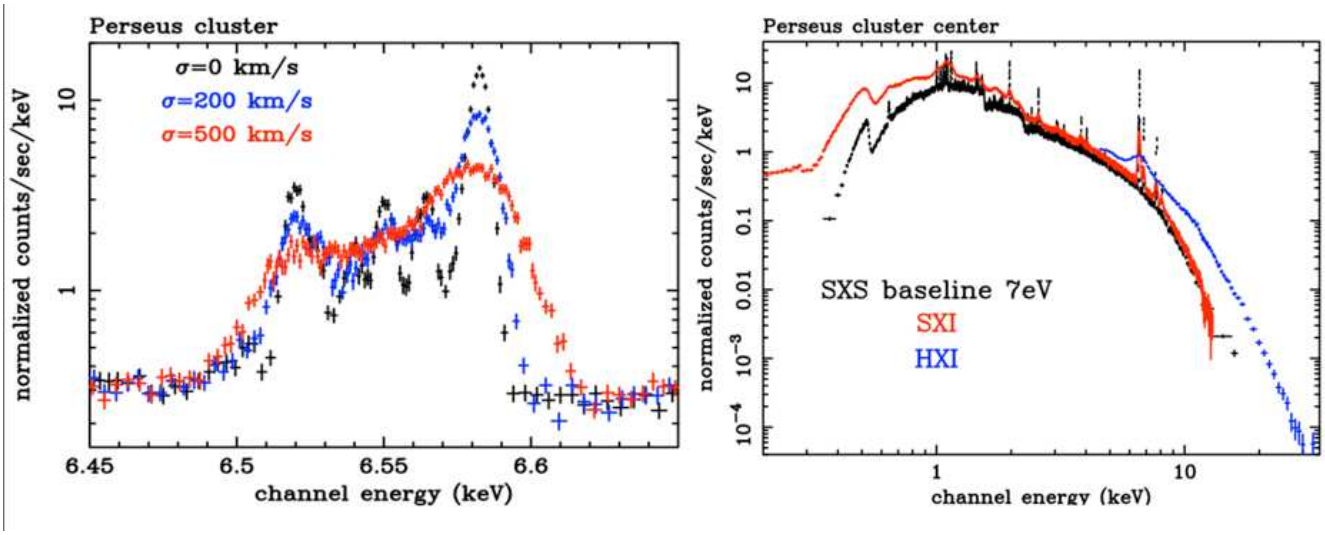


Figure 12. Simulated spectra for 100 ks SXS observation of Perseus Cluster. (left) Line profiles assuming $\sigma$=0, 100 and 200 km/s turbulence. (right) Wide band spectra obtained with SXS and HXI for hot plasma with three different temperature of 0.6 keV, 2.6 keV and 6.1 keV (r < 2' )

ergy equation of state and strong evidence for the existence of dark matter. Using a variety of techniques (including the growth of structure, the baryonic fraction in clusters, and the Sunyaev-Zel'dovich effect) a well-constructed survey of clusters of galaxies, with the necessary supporting data,[42] can provide precise measurements of cosmological parameters, including the amount and properties of dark energy and dark matter. The key step is to connect observables (such as flux and temperature) to cluster masses. Currently, large area cluster surveys are being carried out using the Sunyaev-Zel'dovich Effect by the Atacama Cosmology Telescope, Planck, and the South Pole Telescope to be joined in the near future by the eROSITA X-ray mission. To reduce the systematic uncertainties on the masses inferred from the coarser data from these surveys, a training set of precise cluster masses must be obtained. Measurements of bulk motion of cluster of galaxies and amounts of non-thermal energies going to cosmic-ray acceleration could reduce the "... substantial uncertainties in the baryonic physics which prevents their use at a high level of precision at the present time" (Dark Energy Task Force[43]). Line diagnostics with energy resolution of 7 eV greatly reduce the uncertainties in the baryonic physics by determining the velocity field, any deviations from thermal equilibrium, and an accurate temperature for each cluster. Information about the non-thermal particle content of clusters can be determined via measurements of their Compton upscattering of the CMB: this is best studied via hard X-ray imaging, providing additional clues about the physical state of the cluster gas.

## Acknowledgments

The authors are deeply grateful for on-going contributions provided by other members in the ASTRO-H team in Japan, the US and Europe.

## REFERENCES

[1] NeXT Satellite Proposal,the NeXT working group, submitted to ISAS/JAXA (2005)
[2] NeXT Satellite Proposal,the NeXT working group, submitted to ISAS/JAXA (2003)
[3] H. Kunieda, "Hard X-ray Telescope Mission (NeXT)" , Proc. SPIE, **5488**, p. 187 (2004)
[4] T. Takahashi, K. Mitsuda, & H. Kunieda, "The NeXT Mission" ,Proc. SPIE, **6266**, p. 62660D (2006)
[5] T. Takahashi, et al., "The NeXT Mission", Proc. SPIE, **7011**, 70110O-1 (2008)
[6] SXS Proposal, "High Resolution X-ray Spectroscopy for the JAXA New Exploration X-ray Telescope", NASA/GSFC, submitted to NASA (2007)
[7] M. Kokubun et al., "Hard x-ray imager for the ASTRO-H Mission", Proc. SPIE **7732**, this issue (2010)
[8] K. Mitsuda et al. "The high-resolution x-ray microcalorimeter spectrometer system for the SXS on ASTRO-H", Proc. SPIE **7732**, this issue (2010)
[9] H. Tsunemi et al., "The SXI: CCD camera onboard ASTRO-H", Proc. SPIE **7732**, this issue (2010)
[10] H. Tajima. et al.,"Soft Gamma-ray Detector for the ASTRO-H Mission", Proc. SPIE **7732**, this issue (2010)
[11] H. Kunieda, H. Awaki et al., "Hard X-ray Telescope to be onboard ASTRO-H", Proc. SPIE **7732**, this issue (2010)
[12] P. Serlemitsos et al., "Foil x-ray mirrors for astronomical observations: still an evolving technology", Proc. SPIE **7732**, this issue (2010)
[13] Y. Ogasaka et al., "The NeXT x-ray telescope system: status update", Proc. SPIE, **7011**, 70110P-1 (2008)
[14] H. Kunieda et al., "Balloon-borne hard X-ray Imaging Observation of non-thermal phenomena", Proc. SPIE, **6266**, 62660B (2006)
[15] Y. Ogasaka et al., "Thin-foil multilayer-supermirror hard x-ray telescopes for InFOC$\mu$S/SUMIT balloon experiments and NeXT satellite program", Proc. SPIE **6688**, pp. 668803, 2007.
[16] F. Harrison et al., "Development of the High-Energy Focusing Telescope (HEFT) Balloon Experiment," Proc. SPIE, **4012**, 693 (2000)
[17] T. Takahashi et al., "Wide band X-ray Imager (WXI) and Soft Gamma-ray Detector (SGD) for the NeXT Mission," Proc. SPIE, **5488**, pp.549-560 (2004)
[18] K. Nakazawa et al., "Hard X-ray Imager for the NeXT Mission", Proc. SPIE, **6266**, p. 62662H (2006)

[19] M. Kokubun et al., "Hard X-ray imager (HXI) for the NeXT mission", Proc. SPIE, **7011**, 70110R-1 (2008)
[20] K. Mitsuda et al. "The X-ray micro calorimeter on the NeXT mission", Proc. SPIE, **7011**, 701102K-1 (2008)
[21] T. Okajima et al., "Soft x-ray mirrors onboard the NeXT satellite", Proc. SPIE, **7011**, 85 (2008)
[22] R. Fujimoto et al., "Cooling system for the soft x-ray spectrometer (SXS) onboard ASTRO-H", Proc. SPIE **7732**, this issue (2010)
[23] P.J. Shirron et al. "Design of a 3-stage ADR for the soft x-ray spectrometer instrument on the ASTRO-H mission", Proc. SPIE **7732**, this issue (2010)
[24] K. Narasaki, et al., "Development of cryogenic system for SMILES", Advances in Cryogenic Engineering, **49B**, pp. 1785-1794 (2004)
[25] C.P. de Vries et al., "Filters and calibration sources for the Soft X-ray Spectrometer (SXS) instrument on ASTRO-H", Proc. SPIE **7732**, this issue (2010)
[26] R.L. Kelley et al., "Ion-implanted Silicon X-Ray Calorimeters: Present and Future", J. Low Temp. Phys., **151**, Nos. 1-2 (April 2008)
[27] F. S. Porter and et al., "The detector subsystem for the SXS instrument on the ASTRO-H Observatory", Proc. SPIE **7732**, this issue (2010) pp.91-94 (2009)
[28] F. S. Porter and et al., "The Astro-H Soft X-ray Spectrometer (SXS) ", AIP Conference proceedings **1185**, pp.91-94 (2009)
[29] V. Decaux et al., "High Resolution Measurement of the $K_\alpha$ Spectrum of Fe XXV-XVIII: New Spectral Diagnostics of Nonequilibrium Astrophysical Plasmas,", ApJ. **482**, 1076-1084 (1997)
[30] T. G. Tsuru et al., "Soft X-ray Imager (SXI) onboard the NeXT satellite", Proc. SPIE, **6266**, p. 62662I (2006)
[31] H. Tsunemi et al., "The SXI: CCD camera onboard the NeXT mission", Proc. SPIE, **7011**, p. 70110Q-1 (2008)
[32] T. Takahashi, T. Kamae, and K. Makishima, "Future Hard X-ray and Gamma-ray Observations."in *New Century of X-ray Astronomy*, ASP **251** 210 (2002)
[33] T. Takahashi, K. Nakazawa, T. Kamae, H. Tajima, Y. Fukazawa, M. Nomachi, and M. Kokubun "High resolution CdTe detectors for the next generation multi-Compton gamma-ray telescope", Proc. SPIE, **4851**, pp. 1228-1235, 2003
[34] H. Tajima, T. Mitani, T. Tanaka, H. Nakamua, T. Nakamoto, K. Nakazawa, T. Takahashi, Y. Fukazawa, T. Kamae, M. Kokubun, G. Madejski, D. Marlow, M. Nomachi, E. do Couto e Silva, "Gamma-ray polarimetry with Compton Telescope," Proc. SPIE,**5488**, pp. 561-571 (2004)
[35] K. Koyama et al., "Evidence for Shock Acceleration of High-Energy Electrons in the Supernova Remnant SN:1006, " Nature, **378**, 255 (1995)
[36] Y. Uchiyama, F. Aharonian, T. Tanaka, T. Takahashi, Y. Maeda, "Extremely fast acceleration of cosmic rays in a supernova remnant," Nature, 449, 576 (2007)
[37] F. A. Aharonian, F., Very high energy cosmic gamma radiation: A crucial window on the extreme universe, World Scientific (2004)
[38] Y. Ueda et al.,"Suzaku Observations of Active Galactic Nuclei Detected in the Swift BAT Survey: Discovery of a New Type of Buried Supermassive Black Holes", ApJ, **664**, pp. L79-L82 (2007)
[39] Y. Ueda et al., "Cosmological Evolution of the Hard X-Ray Active Galactic Nucleus Luminosity Function and the Origin of the Hard X-Ray Background", ApJ, **598**, 886 (2003)
[40] Y. Tanaka, et al., "Gravitationally Redshifted Emission Implying an Accretion Disk and Massive Black-Hole in the Active Galaxy MCG:-6-30-15," Nature, **375**, 659 (1995)
[41] J.N. Reeves et al., "Revealing the High Energy Emission from the Obscured Seyfert Galaxy MCG-5-23-16 with Suzaku," PASJ, **59S**, 301 (2007)
[42] D. Rapetti, S. Allen, A. Mantz, "The prospects for constraining dark energy with future X-ray cluster gas mass fraction measurements,". MNRAS, **388**, pp. 1265-1278 (2008)
[43] A. Albrecht et al., "Report of the Dark Energy Task Force", arXiv:astro-ph/0609591v1 (2006)